

Electronic Supplementary Material (ESI) for Journal of Materials Chemistry A.

This journal is © The Royal Society of Chemistry 2019

## ARTICLE

### Supporting Information

## Methylamine-Assisted Secondary Grain Growth for $\text{CH}_3\text{NH}_3\text{PbI}_3$

### Perovskite Film with Large Grains and Highly Preferred Orientation

Haochen Fan<sup>a,b</sup>, Jin-Hua Huang<sup>\*a</sup>, Longsheng Chen<sup>a</sup>, Yue Zhang<sup>a</sup>, Yang Wang<sup>a</sup>, CaiYan Gao<sup>a</sup>, Pengcheng Wang<sup>a</sup>, Xueqin Zhou<sup>b</sup>, Ke-Jian Jiang,<sup>\*</sup> and YanLin Song<sup>\*a</sup>

#### Experimental Details

**Materials.** lead (II) iodide (99.999%) was purchased from Sigma Aldrich. Methylammonium chloride, methylammonium bromide (>99.5%), methylammonium iodide (>99.5%) and Spiro-OMeTAD were purchased from Xi'an Polymer Light Technology in China.

**Fabrication of  $\text{TiO}_2$  electrode.** FTO glasses (TECA7, 6-8  $\Omega/\square$ , NSG, Japan) were cleaned with deionized water, alcohol, and acetone successively via ultrasonic process, and then cleaned with ultraviolet ozone for 10 min. A 30 nm  $\text{TiO}_2$  blocking layer was deposited on the FTO by spray pyrolysis at 450 °C from a precursor solution of 20 mM titanium diisopropoxide bis(acetylacetonate) solution. A 150 nm mesoporous  $\text{TiO}_2$  layer was spin-coated on the substrate with a diluted  $\text{TiO}_2$  paste (18NR-T, Dyesol) in ethanol with a weight ratio of 1:6, and then calcined at 500 °C for 30 min in air.

**Methylamine-assisted secondary grain growth of  $\text{MAPbI}_3$  film.** The starting  $\text{MAPbI}_3$  perovskite films were deposited the  $\text{TiO}_2$  electrode using the conventional one-step anti-solvent method, where a 47 wt.%  $\text{PbI}_2$ :MAI (molar ratio 1:1) solution in *N,N*-dimethylformamide was spin-coated at 4000 rpm for 30 s, quickly dropped 110  $\mu\text{l}$  anhydrous chlorobenzene onto the substrate, followed by a heat-treatment at 100 °C for 10 min. The pristine perovskite film was loaded face up in a closed chamber (as shown in Fig. S1). Before the loading, the chamber preheated in an oil bath pot for 1 hour to ensure that the gas temperature in the reactor reaches the set value and a beaker with a mixture of methylammonium chloride, sodium hydroxide and CaO dryer was loaded in advance for the generation of  $\text{MA}^0$  gas. The CaO is used here to absorb the water from the solid state reaction. The pressure can be adjusted by the valve on the chamber. After the degassing, the sample was taken out. Both the control and the MSGG-based perovskite films were coated by 5 mM of phenylammonium iodide in propanol with 3000 rpm and the film was heated at 100 °C for 1 min.

**Fabrication of solar cells** On the resulting perovskite film, a HTM was deposited by spin coating a solution, which was prepared by dissolving 72.3 mg (2,29,7,79-tetrakis(*N*, *N*-di-*p*-methoxyphenylamine)-9,9-spirobifluorene) (spiro-MeOTAD), 28.8 ml 4-*tert*-butylpyridine, 17.5 ml of a stock solution of 520 mg ml<sup>-1</sup> lithium bis(trifluoromethylsulfonyl)imide in acetonitrile. Finally, 80 nm of gold was thermally evaporated on top of the device to form the back contact.

**Measurement and characterization** The absorption spectra were collected using a UV/Vis spectrometer (SHIMADZU, UV-1800 UV/Vis Spectrophotometer) in the wavelength range of 300–1000 nm. Steady-state photoluminescence (PL) was measured using Edinburgh FLS980 system with an excitation at 485 nm. The powder XRD patterns and rocking curves were measured using a PANalytical Empyrean X-ray powder diffractometer equipped with a 2.2 kW Cu  $\text{K}\alpha$  radiation (1.54 Å). The SEM images were taken from a Hitachi SU8020 SEM operated at 5 kV. Electron backscatter diffraction (EBSD) patterns were acquired by Symmetry EBSD detector of Oxford Instruments on a Hitachi SU5000 SEM. In the measurement, the focused electron beam illuminated at an angle of 70° to the surface of the

perovskite film, and the diffraction patterns (Kikuchi patterns) were collected by the detector, where the beam current was 15 nA at 20 kV with a pixel exposure time of 1 ms. and analyzed using AZtec and Channel 5 software.

Current–voltage ( $J$ – $V$ ) characteristics were recorded by applying an external potential bias to the cell while recording the generated photocurrent with a Keithley model 2400 digital source meter. The light source was a 300 W collimated xenon lamp (Newport) calibrated with the light intensity to 100 mW cm<sup>-2</sup> under AM 1.5G solar light conditions by a certified silicon solar cell. The  $J$ – $V$  curve was recorded by the reverse scans with a rate of 100 mV s<sup>-1</sup>. The active area was determined by metal shadow mask with an aperture of 0.0725 cm<sup>2</sup>. The incident photon-to-current conversion efficiency (IPCE) for solar cells was performed using a commercial setup (PV-25 DYE, JASCO). A 300 W Xenon lamp was employed as a light source for the generation of a monochromatic beam. IPCE spectra were recorded using monochromatic light without white light bias. Calibrations were performed with a standard silicon photodiode.

**Device stability testing.** The humidity stability for both the unencapsulated perovskite films and the relative devices was conducted in a temperature-humidity chamber (DHS-100, Beijing Zhongkehuanshi Instrument Co. Ltd., China). In the experiment, the temperature is maintained at 30 °C with relative humidity 40%. The photovoltaic performance of the aged devices was measured under ambient conditions.

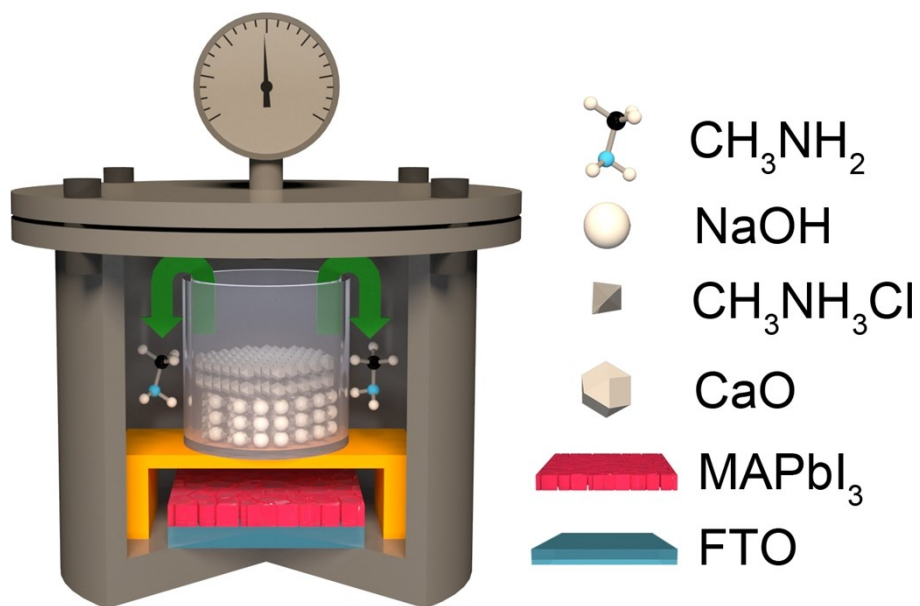
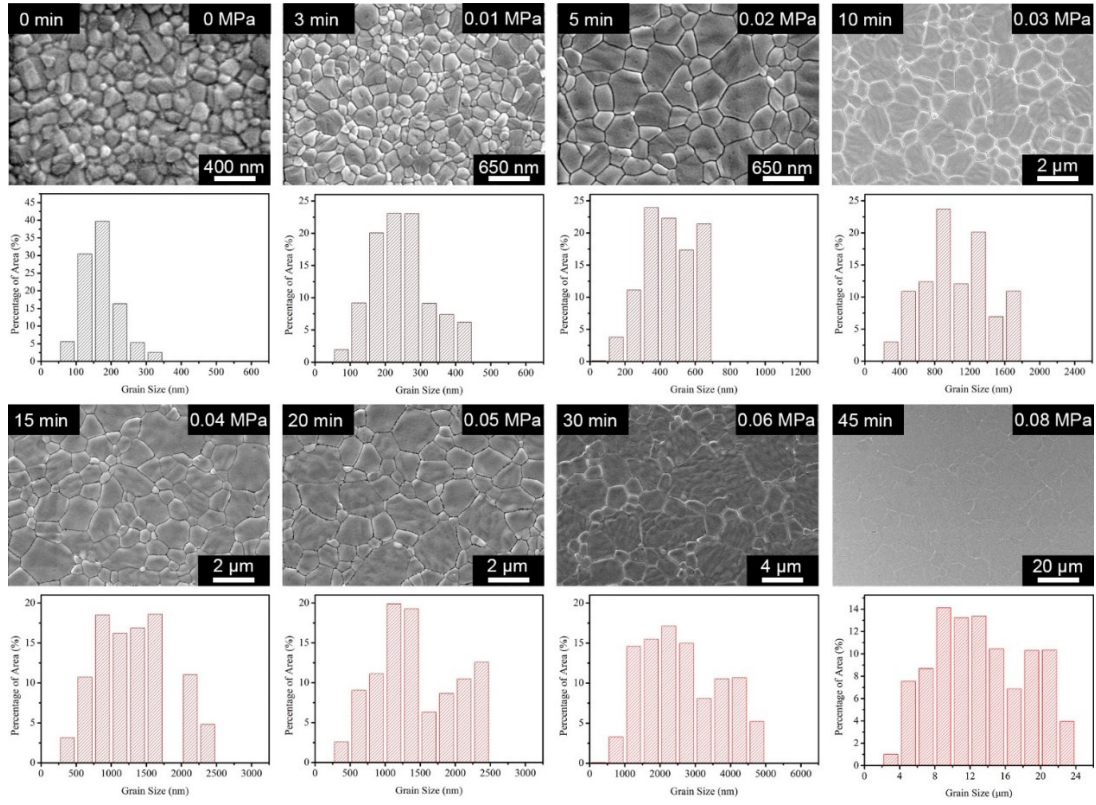
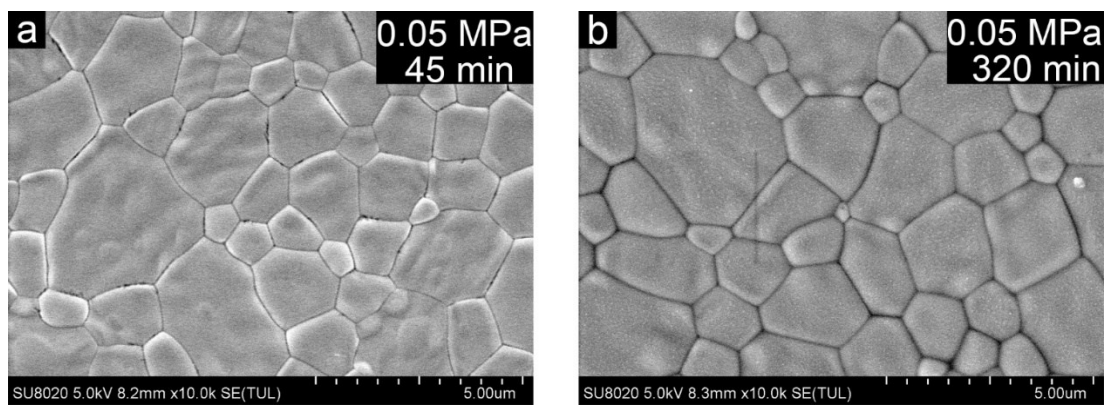


Fig. S1. Schematic diagram of the reaction device.



**Fig. S2.** The SEM images and the corresponding grain size distribution of the MSGG films processed at different reaction intervals, where the corresponding partial pressure of MA<sup>0</sup> ( $P_{MA}$ ) is included for each sample.



**Fig. S3.** The SEM images of the MSGG perovskite films processed at the same temperature of 120 °C with different annealing times.

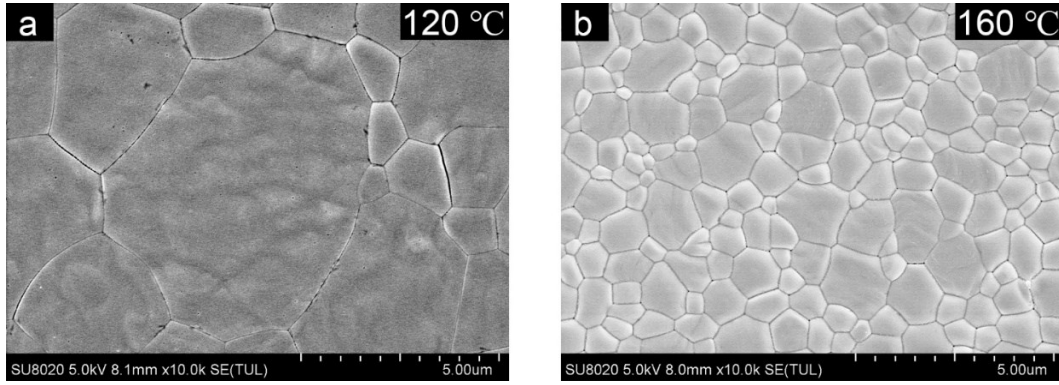


**Fig. S4.** The SEM images of the MSGG film processed at different temperatures with the same  $P_{MA}$ . ( $P_{MA} = 0.06$  MPa).

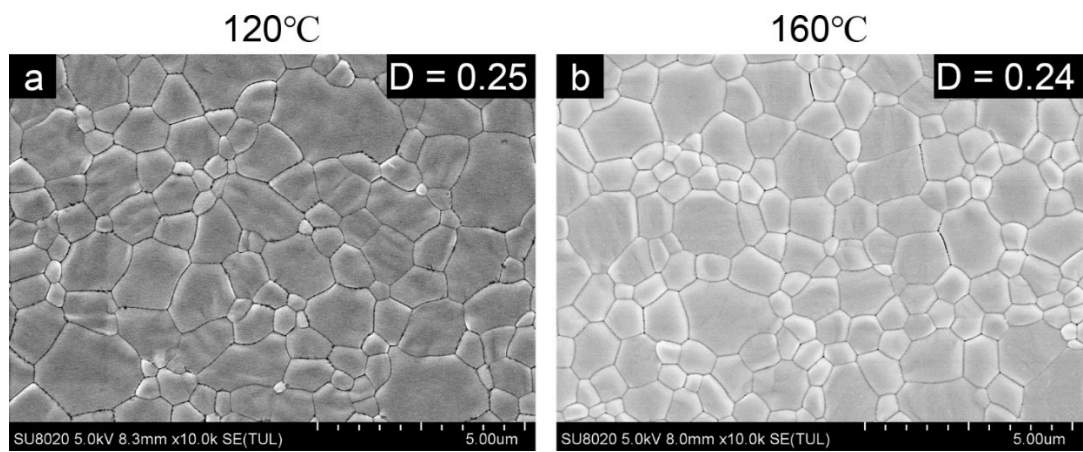


**Fig. S5.** The SEM images of the MSGG films processed at different temperatures with similar  $D$  values.

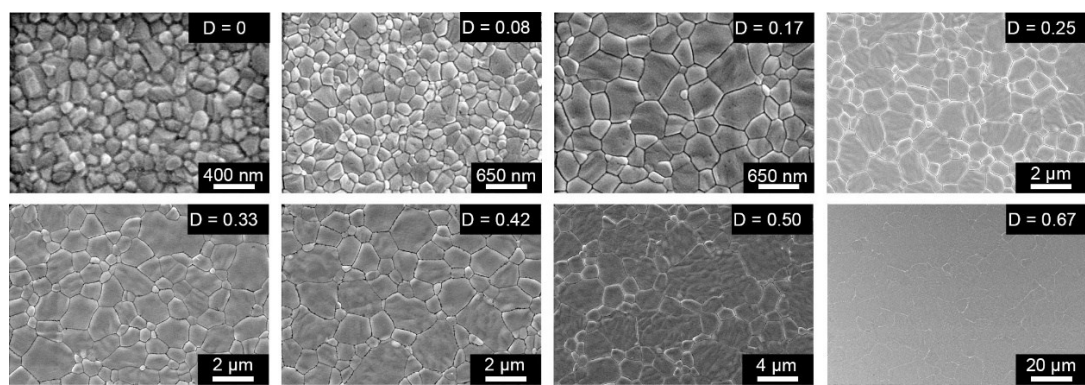


**Fig.S6.** The SEM images of the MSGG films processed at different  $D$  values.



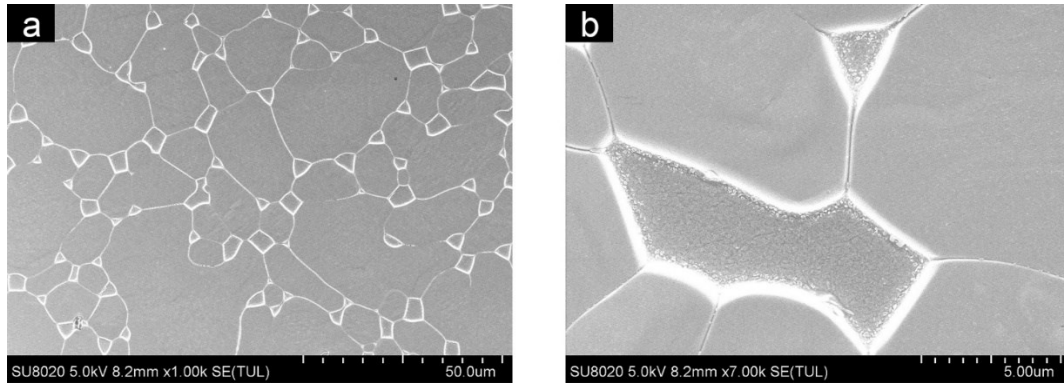


**Fig. S7.** The SEM images of the MSGG film at 120 °C with  $P_{MA} = 0.11$  MPa ( $D = 0.92$ ).

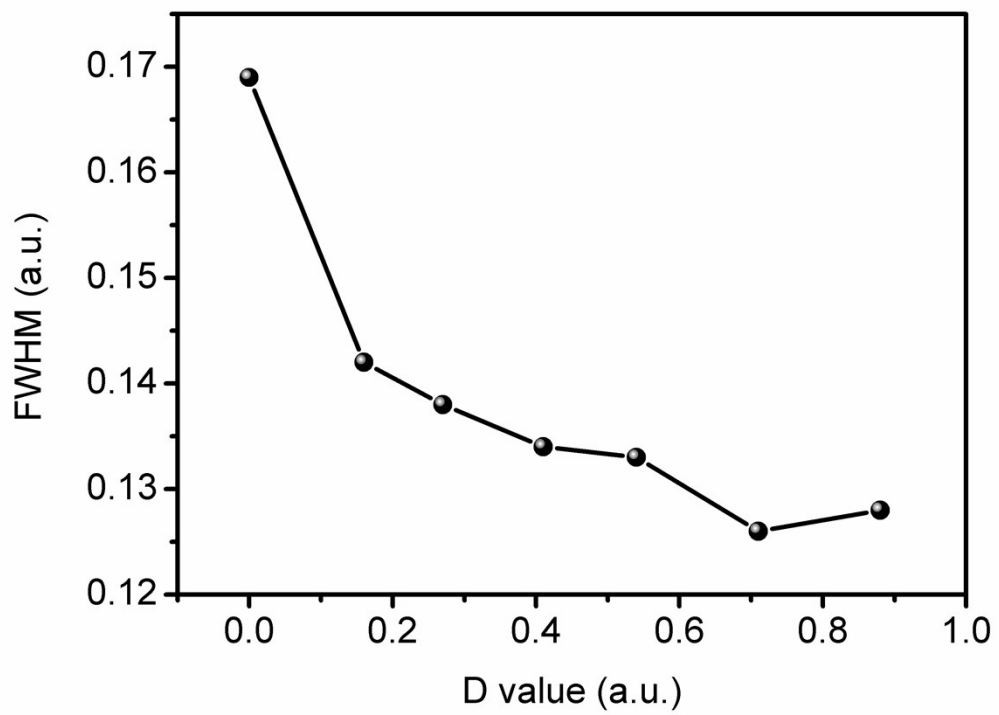


**Fig. S8.** The graph of the FWHM of 110 crystal plane changing with D value.

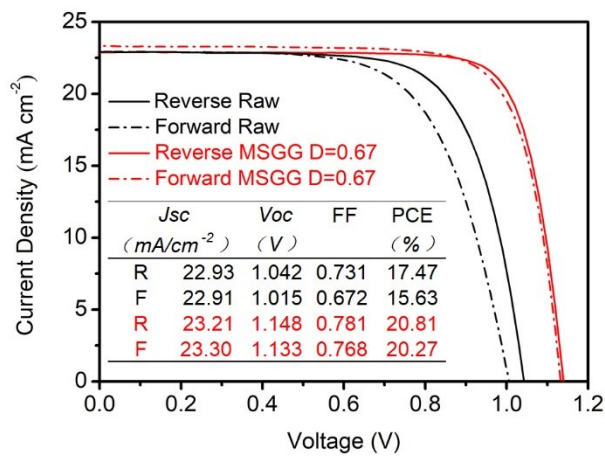


**Fig. S9.** The characteristic  $I$ - $V$  curves of the devices with the raw and MSGG perovskite films. The solid lines and dashed lines indicate the reverse- and forward-bias scan directions, respectively.

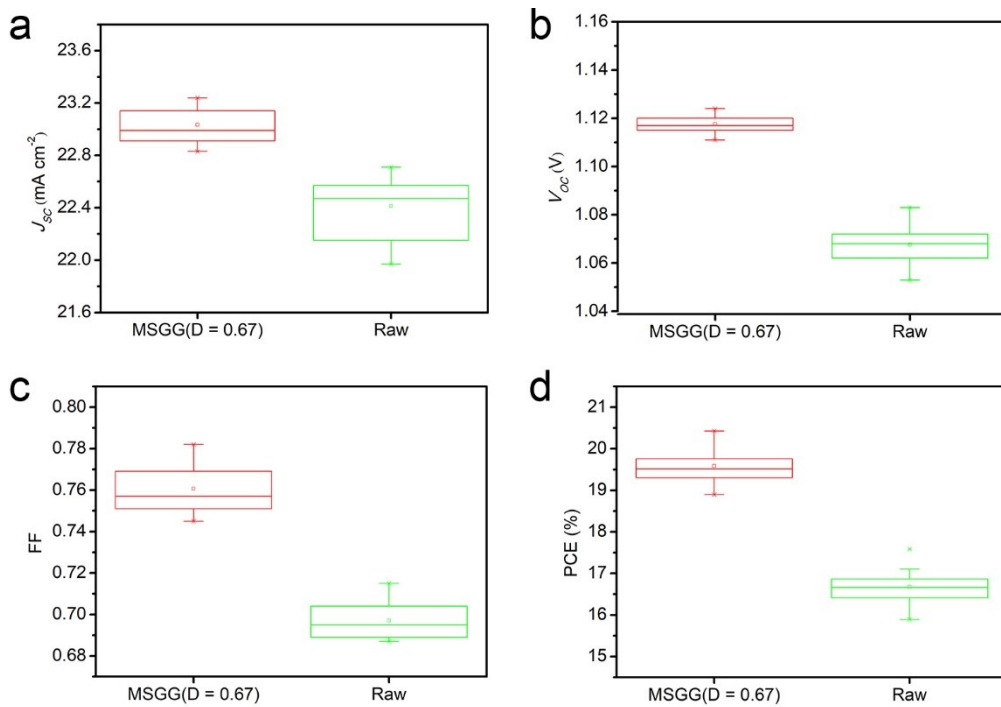


**Fig. S10.** Performance parameters of perovskite solar cell for 20 devices using the raw and the MSGG MAPbI<sub>3</sub> films. (a) Short-circuit current density ( $J_{sc}$ ). (b) Open-circuit voltage ( $V_{oc}$ ). (c) FF. (d) PCE. In the boxplots, the star represents the maximum and minimum values, and the open square represents the mean value.

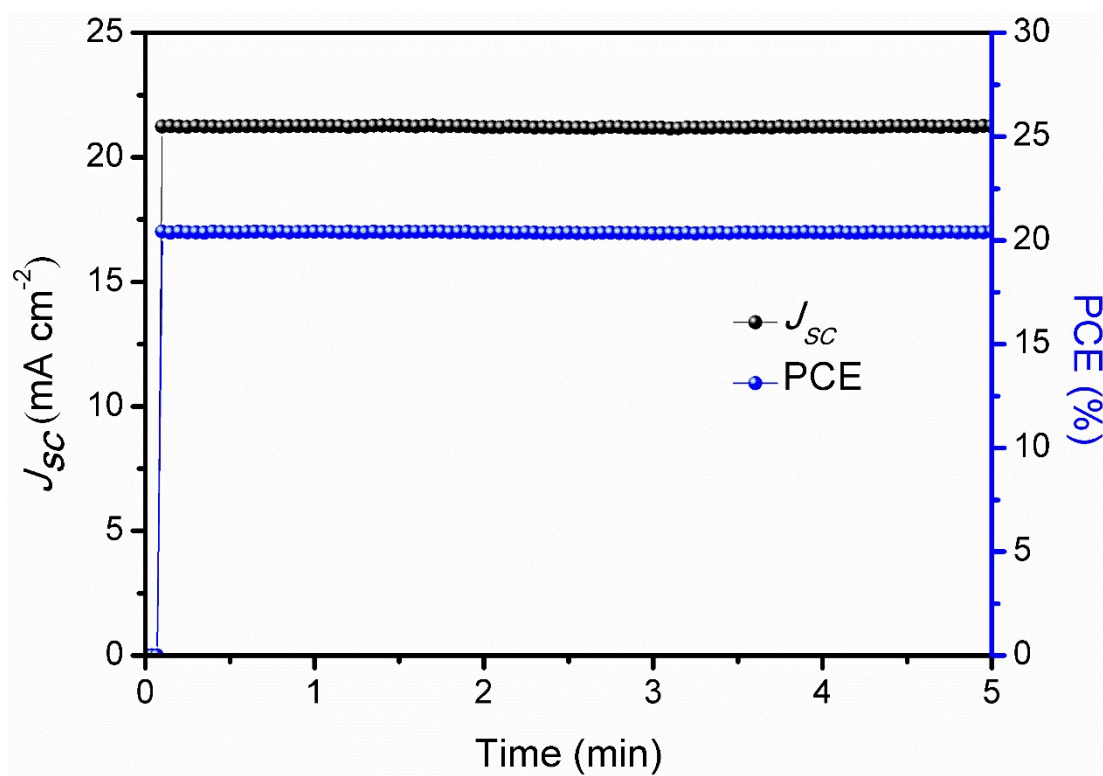


**Fig. S11.** Stabilized maximum power output measurement of the MSGG device with bias at the maximum power point